Geology

How do turbidity flows interact with contour currents in unidirectionally migrating deep-water channels?

--Manuscript Draft--

Manuscript Number:	G40204R1
Full Title:	How do turbidity flows interact with contour currents in unidirectionally migrating deep-water channels?
Short Title:	The interplay of turbidity and contour currents
Article Type:	Article
Keywords:	Turbidity flows; contour currents; deep-water channels
Corresponding Author:	Chenglin Gong Department of Geological Sciences, Jackson School of Geosciences, University of Texas Austin, Texas UNITED STATES
Corresponding Author Secondary Information:	
Corresponding Author's Institution:	Department of Geological Sciences, Jackson School of Geosciences, University of Texas
Corresponding Author's Secondary Institution:	
First Author:	Chenglin Gong
First Author Secondary Information:	
Order of Authors:	Chenglin Gong
	Yingmin Wang
	Michele Rebesco
	Stefano Salon
	Ronald Steel
Order of Authors Secondary Information:	
Manuscript Region of Origin:	CONGO
Abstract:	Inspired by the two-layer model of a stratified lake forced by wind stress, we introduce the concept of Wedderburn number (W) to quantify, for the first time, how turbidity and contour currents interacted to determine sedimentation in unidirectionally migrating deep-water channels (UCs). Bankfull turbidity flows in the studied UCs were computed to be supercritical [Froude number (Fr) of 1.11-1.38] and had velocities of 1.72-2.59 m/s. Contour currents with assumed constant velocities between 0.10 and 0.30 m/s flowing through their upper parts would result in pycnoclines between turbidity and contour currents, with amplitudes of up to 7.07 m. Such pycnoclines, in most cases, would produce Kelvin-Helmholtz (K-H) billows and bores that had velocities of 0.87-1.48 m/s and prograded toward the steep channel flanks by 4.0° to 19.2°. Their wavefronts with the strongest shocks and deepest oscillations would, therefore, occur preferentially along the steep flanks, thereby promoting erosion; on the other hand their wavetails with the weakest shocks and shallowest oscillations would occur preferentially along the gentle flanks, thereby promoting deposition. Such asymmetric intra-channel deposition, in turn, forced individual channels to consistently migrate toward the steep flanks, forming channels with unidirectional channel trajectories and asymmetrical channel cross-sections.

Dear Editor of Geology,

We thank you for considering publishing our manuscript entitled '*How do turbidity flows interact with contour currents in unidirectionally migrating deep-water channels?'* (Ms. No. TG40204). Journal editor (Dr. James Schmitt) and two very well qualified reviewers (Drs. Joris Eggenhuisen and Octavio E. Sequeiros) provided very insightful and constructive comments, all of which significantly improved the final quality of our manuscript. We have systematically addressed the minor revisions suggested, which was helped by strong parallels in their suggestions. Our detailed responses to the suggestions and comments made by the journal Editor and reviewers are listed below.

Yours sincerely,

Chenglin Gong

Corresponding Author
College of Geosciences, China University of Petroleum (Beijing),
18 Fuxue Road, Changping, Beijing 102249, China
E-mail: chenglingong@hotmail.com

Response to comments listed in the formatted and reference-checked manuscript

(1). Comments: In line 43: [[The in-text citation "He et al., 2013" is not in the reference list. Please correct the citation, add the reference to the list, or delete the citation.]] ()

In line 95: [[The in-text citation "He et al., 2013" is not in the reference list.]]

In line 248: [[The in-text citation "He et al., 2013" is not in the reference list.]]

Response: "He et al., 2013" has been deleted, considering we must shorten the overall length of our manuscript.

(2). Comments: In line 43: [[The in-text citation "Palermo et al., 2014" is not in the reference list. Please correct the citation, add the reference to the list, or delete the citation.]]

In line 93: [[The in-text citation "Palermo et al., 2014" is not in the reference list.]]

In line 246: [[The in-text citation "Palermo et al., 2014" is not in the reference list.]]

Response: "Palermo et al., 2014" is a very important reference, and was thus added to the reference list.

(3). Comments: In line 129: [[No figure matches the in-text citation "Figs. 4A and 4B". Please supply a figure and figure caption or delete the citation.]]

In line 133: [[No figure matches the in-text citation "Fig. 4A". Please supply a figure and figure caption or delete the citation.]]

In line 134: [[No figure matches the in-text citation "Fig. 4A".]]

[[No figure matches the in-text citation "Figs. 4A and 4B".]]

[[No figure matches the in-text citation "Figs. 4A and 4B".]]

In line 228: [[No figure matches the in-text citation "Figs. 4A and 4B".]]

In line 257: [[No figure matches the in-text citation "Figs. 4A and 4B".]]

Response: According to comments by journal editor, we moved Figure DR1 out of the Data Repository, which is now Figure 4. We, therefore, updated the order of our figure citations accordingly. We would like to further work on this point if necessary.

Response to comments made by journal editor of Dr. James Schmitt

(1). Comments: There are several additional important issues that must be addressed when you revise the manuscript. These include:

1) Figure DR1 is referred to in the main body of the manuscript numerous times, suggesting that it is fundamental to the reader understanding the interpretations presented therein. Thus, it needs to be incorporated into the main manuscript as a figure (i.e. moved out of the Data Repository). Only supplemental materials should be located in the Data Repository. This will likely involve condensing some text and perhaps combining or reconfiguring figures.

Response: Taking the above comments, we moved Figure DR1 in the previous version out of the Data Repository, which now become Figure 4 of our manuscript. We updated our figure citations throughout the whole text manuscript accordingly.

(2). Comments: 2) Figure 4 is referenced in numerous places in the manuscript, but there is no Figure 4. This discrepancy needs to be addressed and fixed.

Response: The same comments have also been listed in the formatted and reference-checked manuscript. Please refer to our responses to (3). Comments in the annotated manuscript for full details of how we addressed this point in the revised version of our manuscript.

(3). Comments: 3) The English grammar needs to be improved throughout the manuscript. Acquiring grammatical editing help in this regard from a native English speaker may be very helpful.

Response: According to the above comments, we invited my postdoctoral supervisor of Prof. Ron J Steel at the Jackson School of Geosciences of UT Austin to further polish the wording and grammar of our manuscript. Prof. Steel also made some insightful and constructive comments and suggestion during the early stage. We, therefore, added him as one of our coauthors.

Response to comments made by Reviewer #1 of Dr. Joris Eggenhuisen

(1). Comments: The authors establish, for the first time, a quantitative framework that integrates the topics of oceanic contour currents and turbidity currents. They demonstrate how their parameterisations can explain the morphological evolution of prominent features on the ocean floor and in deep water stratigraphy. The paper truly treads new ground, which is a rare accomplishment in this day and age. The discussion is balanced and convincingly calls for new research activity. I enthusiastically encourage *Geology* to publish this paper. Below are some comments regarding final clarifications that I suggest to be beneficial for the paper.

1) The flow condition estimates have been considerably improved. The clarity of the main text has been drastically improved. Many of the secondary variable estimates have been successfully moved to the supplementary materials. With regard to this theme I have the following remaining comments:

- There are now multiple ranges for Ut and Fr in the text and the supplementary materials (cf. L114 and supplementary material). This will make the readers doubtful about the rigour of the quantifications. Please run through all calculations and the text, and ensure that a single, final, consistent set of results is presented throughout.
- It seems that the thickness of the upper layer determines the amplitude of the pycnocline (Eq. 8) but h1 is not defined in the text. This leads the reader to speculate whether this is the thickness of the South Equatorial Current. Please explain and state which value was used for h1.
- The use of h1' is clear in the wind-shear context of the Wedderbrun number; the depth of the interface beneath the wind-shear surface [h1=h1' in the context of wind-shear pycnoclines]. But this is not clear in the contour-turbidity current interaction setting. Please explain what value for h1' is used, and what its interpretation is in this new application.

Response: According to the above comments, we made the following revisions:

Firstly, we double checked ranges for U_t and Fr. A single, final, consistent set of results of U_t and Fr is now presented throughout the text and the supplementary materials, which are listed as follows:

- Velocities of bankfull turbidity currents in the studied channels = 1.72–2.89 m/s (averaging 2.29 m/s);
- Velocities of K-H billows and bores = 0.87–1.48 m/s (averaging 1.17 m/s);
- Fr of bankfull turbidity currents in the studied channels = 1.11–1.38 m/s (averaging 1.24 m/s).

Secondly, we deleted our expression related to h1, in order to avid the confusion. Instead, we employed Shintani et al. (2010) to indicate how amplitude of the deflections of pycnoclines between turbidity and contour currents can be calculated.

(2). Comments: 2) L142-146 This extra determination of deltarho with a bottom friction estimate and a Froude condition is obsolete and overly complicated, as rho1 and rho2 have already been established with much simpler Eq. 4 in lines 135-141. Cut this text, and use 1025 and 1041 kg/m3.

Response: Taking the above comments, Lines 142 to 146 were deleted accordingly.

(3). Comments: 3) There are some remaining doubts about the characteristic velocities to be used in the parameterisations. This is understandable, because the authors use them on combined flows, while these parameters were originally developed on simple flows. I have the following remaining questions:

- -shouldn't the velocity scale in Eq. 7 be the differential velocity between the turbidity current and contour currents?
- -L188-193. I am doubtfull about this velocity scale. The shear between the turbidity current and the contour current is between the maximum velocity and the contour current, surely?

Response: On the basis of the above comments, we followed two lines of revision.

Firstly, we used the same units for both turbidity and contour currents.

Secondly, we softened our wording of Line 188 to 193 accordingly. We indicated that a representative velocity at the interface between turbidity and contour currents is poorly constrained.

(4). Comments: 4) The supplementary material needs to be brought up to the same level as the main text. Dimensionless slope is still reported to be up to 0.4964 [-]; and velocities and Froude numbers are much too high. Roughness is varied up to 1 m; which is a huge value, implying that there are multi-m high bedforms with detached flow cells on the bed. Please clarify this assumed range.

5) Inconsistencies remain in the notation used for variables. These have to be corrected before publication:

Response: We carefully went through our supplementary materials, and made all variables and noteworthy into a single, final, consistent set of results.

(5). Comments: L97 S, not Fr.

L130 & 135: L, not B

L175&176: A, not etha0?

L194-193 Please use consistent typography for V/v.

Suppl page 2: "Densimetric Froude number, not normal density Froude number.

Suppl page 3: ks and kappa s are used for roughness; ks is more common in literature.

Notation: Fr' for the densimetric Froude number; not Fr

Response: We accepted the above suggestions, and corrected our manuscript accordingly.

(5). Comments: 6) The text is not written by native English writers. It is also clear that I am not the best person to suggest all appropriate corrections as my English is certainly not more eloquent. Below I have indicated some occurrences in the text where I feel the text should be rephrased to improve the English style and grammar:

L35-40 Re-order sentence parts.

L123 "The Wedderbrun number…"

L185-186 Rephrase.

Further minor comments:

L56 "runoff mm/yr" Either the rainfall rate in mm/yr, or the runoff in m3/yr.

L104, 114 and other occurrences: The uncertainties in these estimation workflows make reporting 3 significant digits troublesome. I strongly suggest 1.1, 11.4, 1.7, 2.9 as opposed to 1.11, 1.38, etc. Also L180 W-1=4.1 instead of 4.09, etc.

L133 "to", not "to to"

L146-147 L is indicated in Fig 3, not in Fig. 2.

L275 “analyse” not analyis

Response: We reconstructed the above sentences. My postdoctoral supervisor of Prof. Ron J Steel at UT Austin carefully went through the whole text manuscript, and further improved the wording and grammar of our manuscript.

In addition, we used the same level of precision in two significant digits, but are willing to further build our manuscript if necessary.

Response to comments made from Reviewer #2 of Dr. Octavio E. Sequeiros

(1). Comments: Reviewer #2: I have read the authors replies to my original comments and looked into the new version of the manuscript. I have only two further comments. After they are addressed, and I think the authors can do it, I recommend this manuscript for publication:

1) One of my main comments was:

If the hypothesis that unidirectional migrating submarine channels (UCs) are caused by the interaction between oceanic countercurrents and turbidity currents below them is correct, it should be observed ONLY in water depths shallower than those reached by oceanic counter currents. Is this true?

The manuscript focus on a small area of the former continental slope. Is there any evidence that further downstream in deeper waters the submarine channels DO NOT migrate laterally?

Can you find some evidence in the paper you cite? E.g. Merciera et al (2003)?
The authors must address this point.

The authors reply that "we revisited our seismic database, and confirmed that our channels laterally migrated throughout their life span along their entire length."

I was expecting that further downstream the canyons did not migrate laterally. If they do this implies that in the deeper downstream stretches of the canyons, where the oceanic countercurrents do not reach, something else has to explain the lateral migration of the submarine channels.

I believe the authors try to explain this paradox by changes in sea levels during different geological eras.

Thus in another section entitled "GEOLOGICAL AND OCEANOGRAPHIC BACKGROUND" the authors make this statement to support their hypothesis "The documented UCs occur in paleo-water depth of 200 to 500 m, suggesting that the south equatorial currents with an effective depth of 350 m were most likely involved in their construction (Fig. 1; Merciera et al., 2003)."

But still I think you need to be more explicit and state that this is the reason why lateral migration happens in the entirety of the submarine channels. Otherwise readers are going to be confused or misread your text and think that the lateral migration in deeper waters could be happening even now.

If your explanation is right, then you have to state that lateral migration of canyons should happen in present days only in shallow waters, and the lateral migration observed in deeper waters happened in the past, when those sections of the channel where in shallower waters. At least that is how I understand your explanation. But I am not sure if I understand your text correctly. Please be more explicit about this because it is an important point.

Response: Taking the above comments, we made the following revisions.

Firstly, as suggested by Dr. Octavio E. Sequeiros, we find some evidence in previous studies, which suggest that Lower Congo channels in water depth of > the effective depth of south equatorial currents do not have unidirectional trajectories. We added this point to our manuscript accordingly.

Secondly, we gave a short explanation of why lateral migration happens in the entirety of the documented channels in section, entitled “GEOLOGICAL AND OCEANOGRAPHIC BACKGROUND”.

Please refer to section, entitled “GEOLOGICAL AND OCEANOGRAPHIC BACKGROUND” for full details of how we addressed the above comments in our resubmission.

(3). Comments: 2) In the new manuscript line 265 now reads "Thirdly, it is now widely acknowledged that turbidity currents are short (a few days per year), local and intense,…" I think this is generally a valid statement, but a recent paper by Azpiroz-Zabala et al (2017) on the Congo Canyons turbidity currents found that that particular submarine channel is much more active than average and turbidity currents occur quite frequently. I think this supports your hypothesis, so you should mention it.

Azpiroz-Zabala, M., M. J. Cartigny, P. J. Talling, D. R. Parsons, E. J. Sumner, M. A. Clare, S. M. Simmons, C. Cooper, and E. L. Pope (2017), Newly recognized turbidity current structure can explain prolonged flushing of submarine canyons, Science advances, 3(10), e1700,200.

Response: We added the above reference accordingly.

Publisher: GSA
Journal: GEOL: Geology
DOI:10.1130/G40204.1

How do turbidity flows interact with contour currents in unidirectionally migrating deep-water channels?

Chenglin Gong[1,2], Yingmin Wang[2,3], Michele Rebesco[4], Stefano Salon[4], and Ronald J. Steel[5]

[1] State Key Laboratory of Petroleum Resources and Prospecting (China University of Petroleum, Beijing), Changping, Beijing 102249, China

[2]College of Geosciences, China University of Petroleum (Beijing), Changping, Beijing, 102249, China

[3]Ocean College, Zhejiang University, Hangzhou, Zhejiang, 310058, China

[4]Istituto Nazionale di Oceanografia e di Geofisica Sperimentale (OGS), Borgo Grotta Gigante 42/C, 34010 Sgonico, Trieste, Italy

[5]Department of Geological Sciences, Jackson School of Geosciences, University of Texas, Austin, Texas 78712, USA

ABSTRACT

Inspired by the two-layer model of a stratified lake forced by wind stress, we introduce the concept of Wedderburn number (W) to quantify, for the first time, how turbidity and contour currents interacted to determine sedimentation in unidirectionally migrating deep-water channels (UCs). Bankfull turbidity flows in the studied UCs were computed to be supercritical [Froude number (Fr) of 1.11–1.38] and had velocities of 1.72–2.59 m/s. Contour currents with assumed constant velocities between 0.10 and 0.30 m/s flowing through their upper parts would result in pycnoclines between turbidity and contour currents, with amplitudes of up to 7.07 m.

Such pycnoclines, in most cases, would produce Kelvin-Helmholtz (K-H) billows and bores that had velocities of 0.87–1.48 m/s and prograded toward the steep channel flanks by 4.0° to 19.2°. Their wavefronts with the strongest shocks and deepest oscillations would, therefore, occur preferentially along the steep flanks, thereby promoting erosion; on the other hand their wavetails with the weakest shocks and shallowest oscillations would occur preferentially along the gentle flanks, thereby promoting deposition. Such asymmetric intra-channel deposition, in turn, forced individual channels to consistently migrate toward the steep flanks, forming channels with unidirectional channel trajectories and asymmetrical channel cross-sections.

INTRODUCTION

Down-slope turbidity currents and along-slope contour currents are Earth’s most important agents for sediment transport in the world’s oceans (e.g., Rebesco et al., 2014; de Leeuw et al., 2016; Azpiroz-Zabala et al., 2017). Both types of current do not work in isolation, but rather act together in the same place and at the same time (e.g., Gong et al., 2013; Rebesco et al., 2014). In addition to channels created solely by turbidity or contour currents, UCs (*sensu* Gong et al., 2013), reflecting the interaction between the two types of current, are also very common on continental margins (e.g., Gong et al., 2013; Palermo et al., 2014).

In recent years, an increasing effort has been made to understand flow processes and sedimentation in deep-water channels through sedimentological analysis of outcrops, direct measurements of turbidity currents (Azpiroz-Zabala et al., 2017), scaled laboratory experiments (de Leeuw et al., 2016), and numerical approaches (Sequeiros, 2012). To date, however, no study has quantified 3D flow processes and their controls on sedimentation in UCs. The current study quantifies, for the first time, how turbidity and contour currents acted together in UCs.

GEOLOGICAL AND OCEANOGRAPHIC BACKGROUND

The study area is located in the Lower Congo Basin (Fig. 1), which was created by the Early Cretaceous opening of the South Atlantic Ocean (Ho et al., 2012). Vast quantities of clastics were delivered into this basin by the Zaire River with a drainage catchment of 3.8×10^6 km^2 and a sediment load of 4.3×10^7 t/yr (Fig. 1), giving rise to aerially extensive Zaire (Congo) fan (Ho et al., 2012) The studied UCs are Quaternary in age, and occur on the southeastern margin of the Quaternary Zaire fan (Fig. 1).

Three major ocean currents dominate the present-day oceanographic setting of the West African margin, namely Angola coastal current, south equatorial counter current, and south equatorial current (Fig. 1). The very energetic Angola coastal currents and seasonal eastward-flowing south equatorial counter currents predominate on the West African shelf (Fig. 1; Mercier et al., 2003). Northward-flowing south equatorial currents with an effective depth of approximately 350 m, in contrast, dominate mainly on the West African slope (Fig. 1; Mercier et al., 2003). The documented UCs occur in paleo-water depth of 200–500 m, suggesting that the south equatorial currents on the West African slope were most likely involved in their construction (Fig. 1; Mercier et al., 2003). Contour currents generally involve a significant volume of water mass in a large area, and persist over very long time intervals, most likely causing the documented UCs to migrate northward consistently in the direction of the modern northward-flowing south equatorial currents throughout their life span (Figs. 1 and 2). It should be noted that channels on the West African slope with water depth > the effective depth of the south equatorial current do not have unidirectional migration trajectories (Ho et al., 2012).

ESTIMATING BANKFULL TURBIDITY CURRENT CONDITIONS FROM DEEP-WATER CHANNEL MORPHOLOGY

Unidirectionally Migrating Deep-Water Channels in the Lower Congo Basin

Six UCs of Quaternary age were recognized in the Lower Congo Basin (UC1 to UC6 in Fig. 2). In cross-sectional view, they display asymmetrical channel cross-sections with northern channel flanks that are, overall, 1.5–3.5 times steeper than their southern counterparts (Fig. 2). They are composed of a series of seismically resolvable channel-complex sets that have bankfull channel widths of 1506–3817 m and bankfull channel depths of 64–108 m, giving aspect ratios of 16–45 (Table DR1). In plan view, they are represented by alternating sets of closely spaced, crescent-shaped, straight, high- and low-amplitude threads (Fig. 3A), and have mean slope gradient (S) of 0.011–0.020 (averaging 0.015).

Estimating Bankfull Turbidity Current Conditions

The Froude number method of Sequeiros (2012) returns Fr as a function of S, the combined friction factor for turbidity currents $[C_f(1+\alpha)]$, and the ratio of shear velocity to settling velocity (u_*/v_s), express as Equation 1.

$$Fr = [0.15 + \tanh(7.62S^{0.75})](1 + v_s/u_*)^{1.1}[C_f(1+\alpha)]^{-0.21} \quad (1)$$

It is applicable to both sinuous and straight deep-water channels (Sequeiros 2012), and was thus employed to estimate bankfull turbidity current conditions in the studied UCs. Using Equation 1, Fr of turbidity currents in the studied channels was computed to range from 1.11 to 1.38 (averaging 1.24) (see the Data Repository for full details of our computation), thereby displaying supercritical flow regimes (Fig. 4A). The layer-averaged velocity of channel turbidity currents (U_t) was then calculated via Equation 2.

$$U_t = Fr(g\overline{\Delta\rho}/\overline{\rho}h)^{1/2} \qquad (2)$$

where: (i) g is the gravitational acceleration; (ii) $\overline{\Delta\rho}$ refers to the layer-averaged excess density of the current; (iii) $\overline{\rho}$ denotes the layer-averaged density of the turbidity flow; and (iv) $\overline{\Delta\rho}/\overline{\rho}$ signifies the layer-averaged fractional excess density of the flow with respect to that of the ambient fluid (ρ_a) (i.e., $\overline{\Delta\rho}/\overline{\rho}$ of < 0.7% for field-scale turbidity currents, as suggested by Sequeiros, 2012). U_t was then computed to range from 1.72 to 2.59 m/s (Fig. 4B; (see the Data Repository). Cross-plot of our results of *S* and *Fr* against 73 measurements of *S* and *Fr* of turbidity currents has a high correlation coefficient of R^2 = 0.82 (n = 82) (Fig. 4A), validating the accuracy of our computations.

HOW DO TURBIDITY FLOWS INTERACT WITH CONTOUR CURRENTS?

Parameterizing Amplitudes of Pycnoclines between Turbidity and Contour Flows

Wedderburn number (*W*) is widely used in limnology research to estimate wind-forced internal seiche behaviors in lakes (Shintani et al., 2010), and is employed to answer the question of how turbidity flows interact with contour currents in Lower Congo UCs? Tilting displacements of the interface between lower turbidity flows and upper contour currents (i.e., pycnoclines) would normally be parameterized by W:

$$W = \frac{g(\rho_2 - \rho_1)h^2}{\rho_1 \mathrm{v}_*^2 \mathrm{B}} = \frac{g(\Delta\rho)h^2}{\rho_1 \mathrm{v}_*^2 \mathrm{B}} \qquad (3)$$

where: (i) ρ_1 and ρ_2 are densities of upper contour currents and lower turbidity flows, respectively (Fig. 3B); (ii) h denotes the thickness of the turbidity current; (iii) B is bankfull channel width (Fig. 3B); and (iv) v_* refers to to turbulent velocity at the interface between the water masses.

To compute W, four variables (ρ_2, $\Delta\rho$, B, and v_*) were determined. First, Sequeiros (2012) suggested that ρ_2 can be computed by:

$$\rho_2 = \rho_i(1 - C) + \rho_s C \qquad (4)$$

where ρ_i and ρ_s denote density of the interstitial fluid and particles, respectively, and C signifies sediment concentration in the current. Assuming ρ_i = 1025 kg/m^3 and C = 1% being typical of turbidity currents, ρ_2 was then calculated to be 1041 kg/m^3. Second, B was measured from nine chosen channel cross-sections (Table DR1). Third, v_* is derived from the shear stress as $\tau = \rho_1 \mathrm{v}_*^2 = \rho_1 C_d {U_c}^2$ (Shintani et al., 2010), so that:

$$v_* = \sqrt{C_d} U_c \qquad (5)$$

where: (i) C_d is the drag coefficient, and is set by the interfacial environment rate and (ii) U_c is the velocity of the contour currents. U_c is poorly constrained; however, existing data sets suggest that it is in many cases between 0.10–0.30 m/s

(Wetzel et al., 2008). W was then computed to range from 0.21 to 1.04 (when U_c = 0.10 m/s) or to vary from 0.07 to 0.35 (when U_c = 0.30 m/s) (Fig. 4C).

Shintani et al. (2010) have suggested that the amplitude of the deflections of pycnoclines (A) can be estimated by:

$$A = \frac{1}{2W} \qquad (6)$$

Our results suggest that A ranges from 0.48 to 2.36 m, when U_c = 0.10 m/s; or from 1.44 to7.07 m, when U_c = 0.30 m/s (Fig. 4C).

Parameterizing the Internal Wave Field Along Pycnoclines

The internal pycnocline response of turbidity flows in the studied channels to a forcing event of contour currents can be gauged by the new Wedderburn number (W^{-1}) (Boegman et al., 2005), defined as:

$$W^{-1} = \frac{A}{\grave{h}_1} \qquad (7)$$

where: $\grave{h}_1$ is the interface depth. W^{-1} was estimated to range from 0.96 to 4.71, when U_c = 0.10 m/s; or from 2.87 to 14.13, when U_c = 0.30 m/s. Boegman et al. (2005) have suggested that strong forcing (represented by $0.96 < W^{-1}$) would most likely produce Kelvin-Helmholtz (K-H) billows and bores.

Reconstructing K-H Billows or Bores Along Pycnoclines

Supercritical turbidity currents in the studied UCs are typically stratified flows, and thus have their peak velocity near the bed. A representative velocity at the interface of such stratified supercritical flows would, thus, be lower than their layer-averaged or peak velocity. The representative velocity at the interface is poorly constrained, but can be assumed to be $U_t/2$ for maximum (Dr. Octavio E. Sequeiros, pers. comm. 2017). The local paleocurrent velocities (v) and directions (β) of K-H billows and bores were computed by Equation 8 and Equation 9, respectively (Fig. 3B):

$$v = \sqrt{(\frac{U_t}{2})^2 + {U_c}^2} \quad (8)$$

$$\beta = \arctan[U_c/(\frac{U_t}{2})]. \quad (9)$$

Our results suggest that when U_c = 0.10 m/s, v and β were computed to range from 0.87 to 1.45 m/s and 4.0º to 6.6º, respectively (Fig. 4D); or that when U_c = 0.30 m/s, v and β were calculated to range from 0.91 to 1.48 m/s and 11.7º to 19.2º, respectively (Fig. 4D).

HOW DOES THE INTERPLAY OF TURBIDITY AND CONTOUR CURRENTS DETERMINE SEDIMENTATION?

As discussed above, the interplay of turbidity and contour currents in the studied UCs would have produced pycnoclines that had A of 0.48–7.07 m, and likely yielded K-H billows and bores, which propagated toward and impinged the steep channel flanks by 4.0° to 19.2°. They therefore generated the strongest shocks, largest amplitudes, and longest wavelengths at their fronts along the steep flank of any channel. Conversely, the weakest shocks, shallowest oscillations, smallest amplitudes, and shortest wavelengths are expected at their rear along the gentle flank (Figs. 3B and 3C). The steep channel flanks were thus more prone to erosion by turbulent mixing between turbidity and contour currents.

The suggested flow structure of K-H billows and bores with wave fronts along the steep channel flanks versus wave tails along the gentle channel flanks is supported by the following three lines of evidence (Figs. 3B and 3C). First, the Lower Congo UCs display asymmetrical channel cross-sections with steep flanks that are, overall, 1.5–3.5 times steeper than their southern gentle flanks (Fig. 2). Second, high-amplitude seismic reflections suggest sands preferentially accumulated along the steep flanks, whereas low-amplitude seismic reflections indicative of muddier deposits preferentially accumulated along gentle flanks (Fig. 2). Third, steep flanks contain truncation terminations, whereas their gentle flanks exhibit downlap terminations (Fig. 2B). All of these observations collectively point to steep-flank erosion versus gentle-flank deposition (Figs. 3B and 3C). Contour currents generally display predominantly unidirectional flow conditions (Wetzel et al., 2008), suggesting that K-H billows and bores would have persistently promoted steep-flank erosion versus gentle-flank deposition, forcing individual channels to consistently migrate in the direction of the steep flanks through time (Fig. 2, 3B, and 3C).

CONCEPTUAL IMPLICATIONS

Our results provide three main contributions towards better understanding of unidirectionally migrating deepwater channels. Firstly, UCs were recently recognized on the northern South China Sea margin (Gong et al., 2013), and were also well developed in the Lower Congo Basin (Fig. 2) and offshore Northern Mozambique (Palermo et al., 2014). They are, thus, fairly common on continental margins, although they are quite different from well-documented turbidite or contourite channels. This study succeeds in using W to interpret unidirectional along-slope channel migration, and quantifies the pycnocline response of turbidity flows to the forcing of contour currents for the first time, thereby contributing to a more complete picture of flow processes and sedimentation in submarine channels.

Secondly, the general energy differences between turbidity and contour currents have made their interaction one of the most controversial issues since the 1970s (e.g., Rebesco et al., 2014). Our results suggest that, in most cases, pycnoclines between turbidity and contour currents could produce K-H billows and bores that impinged the steep channel flanks (Figs. 3B and 3C). Their shocking wave fronts and deep oscillations promoted steep-flank erosion, whereas their wavetails with shallow oscillations would have promoted gentle-flank deposition. Our results, therefore, help to better understand and provide a new model of the interplay of turbidity and contour currents. Our results, therefore, may set the tone in exploring further quantification of the interplay of oceanic contour currents and the sedimentology of turbidity currents.

Thirdly, it is now widely acknowledged that turbidity currents carry a significant sedimentary load, are brief events (a few days per year), local and intense, and draw the attention of mainly sedimentologists (Azpiroz-Zabala et al., 2017). Conversely, contour currents are essentially clean-water, long-lived (up to millions of years), of great spatial extent, and have the attention mainly of oceanographers (Rebesco et al., 2014). Therefore, turbidity and contour currents are usually not addressed jointly. However, our observations have shown that the depositional/erosional record of some deep-water channels contain clear signals from both turbidity and contour currents, and we advocate closer collaboration between stratigraphic communities that separately analyze turbidity or contour currents.

CONCLUSIONS

We used the concept of Wedderburn Number, for the first time, to quantify pycnocline response of turbidity currents to forcing events of contour currents in widely occurring UCs. Pycnoclines between turbidity and contour currents would be produced when contour currents with boundary current velocities (assumed constant between 0.10 and 0.30 m/s) flowed across the pathway of supercritical turbidity flows in submarine channels with Fr of 1.11–1.38 and U_t of 1.72–2.59 m/s. They had W of 0.07–1.04 and A of up to 7.07 m, and would thus, in most case, have produced K-H billows and bores. These K-H billows and bores had velocities of 0.87–1.48 m/s and impinged toward the steep flanks by 4.0° to 19.2°. Therefore, their wavefronts with the strongest shocks and deepest oscillations would have occurred preferentially along the steep channel flanks, constantly promoting erosion and resultant steep channel walls with common occurrence of truncation terminations. Their wavetails with the weakest shocks and shallowest oscillations, in contrast, would have occurred preferentially along the gentle channel flanks, favoring gentle-flank deposition, and gentle channel walls with widespread downlap stratal terminations. Such asymmetric intra-channel deposition would have persistently forced individual channels to migrate in the direction of the steep flanks through time, as recorded by unidirectional channel-growth trajectories.

ACKNOWLEDGMENTS

This research was jointly funded by the Independent Project of State Key Laboratory of Petroleum Resources and Prospecting (No. PRP/indep-1-1701) and the

Science Foundation of China University of Petroleum, Beijing (No. 2462017YJRC061) to C Gong and by the National Natural Science Foundation of China (No. 41372115) to Y Wang. This study has been significantly improved by comments from journal editor James Schmitt and reviewers of Joris Eggenhuisen and Octavio E. Sequeiros.

REFERENCES CITED

Azpiroz-Zabala, M., Cartigny, M.J., Talling, P.J., Parsons, D.R., Sumner, E.J., Clare, M.A., Simmons, S.M., Cooper, C., and Pope, E.L., 2017, Newly recognized turbidity current structure can explain prolonged flushing of submarine canyons, Science advances, 3: e1700200.

Boegman, L., Ivey, G.N., and Imberger, J., 2005, The degeneration of internal waves in lakes with sloping topography: Limnology and Oceanography, v. 50, p. 1620–1637, https://doi.org/10.4319/lo.2005.50.5.1620.

de Leeuw, J., Eggenhuisen, J.T., and Cartigny, M.J.B., 2016, Morphodynamics of submarine channel inception revealed by new experimental approach: Nature Communications, v. 7, p. 10886, https://doi.org/10.1038/ncomms10886.

Gong, C., Wang, Y., Zhu, W., Li, W., and Xu, Q., 2013, Upper Miocene to Quaternary unidirectionally migrating deep-water channels in the Pearl River Mouth Basin, northern South China Sea: The American Association of Petroleum Geologists Bulletin, v. 97, p. 285–308, https://doi.org/10.1306/07121211159.

Ho, S., Cartwright, J.A., and Imbert, P., 2012, Vertical evolution of fluid venting structures in relation to gas flux, in the Neogene-Quaternary of the Lower Congo

Basin, Offshore Angola: Marine Geology, v. 332–334, p. 40–55, https://doi.org/10.1016/j.margeo.2012.08.011.

Mercier, H., Arhana, M., and Lutjeharms, J.R.E., 2003, Upper-layer circulation in the eastern Equatorial and South Atlantic Ocean in January-March 1995: Deep-sea Research. Part I, Oceanographic Research Papers, v. 50, p. 863–887, https://doi.org/10.1016/S0967-0637(03)00071-2.

Palermo, D., Galbiati, M., Famiglietti, M., Marchesini, M., Mezzapesa, D., and Fonnesu, F., 2014, Insights into a new super-giant gas field - sedimentology and reservoir modeling of the coral complex, offshore northern Mozambique. OTC-24907-MS.

Rebesco, M., Hernández-Molina, F.J., Rooij, D.V., and Wåhlin, A., 2014, Contourites and associated sediments controlled by deep-water circulation processes: State-of-the-art and future considerations: Marine Geology, v. 352, p. 111–154, https://doi.org/10.1016/j.margeo.2014.03.011.

Shintani, T., de la Fuente, A., Niño, Y., and Imberger, J., 2010, Generalizations of the Wedderburn number: Parameterizing upwelling in stratified lakes: Limnology and Oceanography, v. 55, p. 1377–1389, https://doi.org/10.4319/lo.2010.55.3.1377.

Sequeiros, O.E., 2012, Estimating turbidity current conditions from channel morphology: A Froude number approach: Journal of Geophysical Research, v. 117, C04003, https://doi.org/10.1029/2011JC007201.

Wetzel, A., Werner, F., and Stow, D.A.V., 2008, Bioturbation and biogenic sedimentary structures in contourites, *in* Rebesco, M., and Camerlenghi, A., eds., Contourites: Developments in Sedimentology: Oxford, UK, Elsevier, v. 60, p. 183–202, https://doi.org/10.1016/S0070-4571(08)10011-5.

FIGURE CAPTIONS

Figure 1. Google Earth image showing geographical and oceanographic context of the study area in the Lower Congo Basin.

Figure 2. (A) Strike-view seismic section showing cross-sectional seismic expression of six UCs. (B) Strike-oriented seismic line (line locations shown in Fig. 3A) showing a close-up view of Lower Congo UC1 to UC3.

Figure 3. (A) Representative time slice taken 350 ms below the modern seafloor showing plan-view geomorphological expression of UC1 to UC3. (B and C) Schematic illustrations of a simple two-layer model employed to quantify how turbidity and contour currents act together and jointly determined sedimentation in UCs.

Figure 4. Scatterplots of S versus Fr (A), U_t versus z_p/h (B), W against A (C), and $ß$ against V (D).

DOI:10.1130/G40204.1

1GSA Data Repository item 2018xxx, xxxxxxxx, is available online at http://www.geosociety.org/datarepository/2018/ or on request from editing@geosociety.org.

Publisher: GSA
Journal: GEOL: Geology
DOI:10.1130/G40204.1

How do turbidity flows interact with contour currents in unidirectionally migrating deep-water channels?

Chenglin Gong[1,2], Yingmin Wang[2,3], Michele Rebesco[4], Stefano Salon[4], and~~,~~ Ronald J. Steel[5]

[1] State Key Laboratory of Petroleum Resources and Prospecting (China University of Petroleum, Beijing), Changping, Beijing 102249, China

[2]College of Geosciences, China University of Petroleum (Beijing), Changping, Beijing, 102249, China

[3]Ocean College, Zhejiang University, Hangzhou, Zhejiang, 310058, China

[4]Istituto Nazionale di Oceanografia e di Geofisica Sperimentale (OGS), Borgo Grotta Gigante 42/C, 34010 Sgonico, Trieste, Italy

[5]Department of Geological Sciences, Jackson School of Geosciences, University of Texas, Austin, Texas 78712, USA~~;~~

ABSTRACT

Inspired by the two-layer model of a stratified lake forced by wind stress, we introduce the concept of Wedderburn number (*W*) to quantify, for the first time, how turbidity and contour currents interacted ~~act together and~~ ~~acted together and jointly~~ to determined ~~ed~~ sedimentation in unidirectionally ~~(laterally)~~ migrating deep-water channels (UCs). Bankfull turbidity flows in the studied UCs were computed to be supercritical [~~(~~Froude number *(Fr)* of 1.11–1.38~~)~~] and had velocities of 1.72–2.~~59~~ ~~8~~59 m/s. Contour currents with assumed constant velocities ~~assumed constant~~

between 10 and 30 cm/s0.10 and 0.30 m/s flowing on through their upper parts would result in pycnoclines between turbidity and contour currents, with amplitudes of up to 7.07 m. ([represented by W of 2.66)]. Such pycnoclines, in most cases, would produce Kelvin-Helmholtz (K-H) billows and bores and bores (represented by 1.20 << mean value of $W^{-1} = 4.09$) that had velocities of 0.87–1.48 m/s and prograded toward the northern steep flanksthe steep channel flanks by 4.0° to 19.2°. Their wavefronts with the strongest shocks and deepest oscillations would, therefore, occur preferentially along the northern steep flanksthe steep flanks, thereby promoting erosion; on the other hand whereas their wavetails with the weakest shocks and shallowest oscillations would, therefore, occur preferentially along the southern, gentle flanksthe gentle flanks, thereby promoting deposition. Such asymmetric intra-channel deposition, in turn, forced –individual channels to consistently migrate toward northern steep flanksthe steep flanks, forming channelsUCs with unidirectional channel trajectories and asymmetrical channel cross-sections.

INTRODUCTION

Down-slope turbidity currents currents, together witand h along-slope contour currents, – are the Earth's most important agents for sediment transport in the world's oceans (e.g., Rebesco et al., 2014; Peakall and Sumner 2015; de Leeuw et al., 2016; Azpiroz-Zabala et al., 2017). Both types of current doof them are not working in complete isolation, but rathercan act together and cooccur in the same place and at the same time (e.g., Gong et al., 2013; Rebesco et al., 2014). In addition to channels created solely by turbidity or contour currents (turbidite or contourite channels), UCs (*sensu* Gong et al., 2013), reflecting~~produced by~~ the interaction between the two types of~~ turbidity and contour~~ currents, are also very common~~ have also been proven ubiquitous~~ on continental margins ~~as recently reported at several scientific meetings and in some recent papers~~worldwide (e.g., Gong et al., 2013~~; He et al., 2013~~**~~[[The in-text citation "He et al., 2013" is not in the reference list. Please correct the citation, add the reference to the list, or delete the citation.]]~~**; Palermo et al., 2014**~~[[The in-text citation "Palermo et al., 2014" is not in the reference list. Please correct the citation, add the reference to the list, or delete the citation.]]~~**).

In recent years, an increasing effort has been made to understand flow processes and sedimentation in deep-water channels through sedimentological analysis of outcrops~~ (Peakall and Sumner 2015Pyles et al., 2012)~~, direct measurements of turbidity currents (Azpiroz-Zabala et al., 2017~~Peakall and Sumner 2015Parsons et al., 2010~~), scaled laboratory experiments (de Leeuw et al., 2016), and numerical approaches (Sequeiros, 2012). ~~Gong et al. (2016) inferred how bottom currents controlled secondary flow structures in UCc, based on simplified assumptions and 3D seismic data.~~ To date, however, no study has quantified 3D flow processes and their controls on sedimentation in UCs. The current study quantifies, for the first time, how turbidity and contour currents acted together~~ and jointly determined~~ ~~sedimentation~~ in UCs.

GEOLOGICAL AND OCEANOGRAPHIC BACKGROUND

The study area is located in the Lower Congo Basin~~, West African margin~~ (Fig. 1), which was created by the Early Cretaceous opening of the South Atlantic

Ocean (Ho et al., 2012). Vast quantities of clastics were delivered into this basin by the Zaire River with a drainage catchment of 3.8 × 10^6 km^2 and a sediment load of 4.3 × 10^7 t/yr (Fig. 1), giving rise to aerially extensive Zaire (Congo) fan (Ho et al., 2012). The Zaire fan was fed by the Zaire River with a drainage catchment of 3.8 × 10^6 km^2, sediment load of 4.3 × 10^7 t/yr, sediment yield of 1.1 × 10^7 t/km^2/yr, and runoff rate of 340 mm/yr, and extends ~800 km into the Atlantic Ocean (Fig. 1). The studied UCs are Quaternary in age, and occur onat the southeastern margin of the Quaternary Zaire fan (Fig. 1).

Three major ocean currents dominate the present-day oceanographic settings of the West African margin, namelyincluding Angola coastal currents (i.e., longshore drift), south equatorial counter currents, and south equatorial currents (Fig. 1). The very energetic Angola coastal currents and seasonal eastward-flowing south equatorial counter currents longshore drift predominates on the West African shelf, and redistributes sediments northwestward along the upper Congo and Gabon shelves (Fig. 1; Stramma and England, 1999; Mercier et al., 2003). Northward-flowing south equatorial currents have with an effective depth of approximately 350 m and a velocity of up to 0.10 10 cm/s, in contrast, dominate mainly on the West African slope (Fig. 1; Stramma and England, 1999; Mercier et al., 2003). The documented UCs occur in paleo-water depth of 200–500 m, suggesting that the south equatorial currents dominated on the West African slope were most likely involved in their construction (Fig. 1; Mercier et al., 2003). Contour currents generally involve a significant volume of water mass in a large area, and persist over very long timelong -

Publisher: GSA
Journal: GEOL: Geology
DOI:10.1130/G40204.1

time intervals, most likely causing the documented UCs to migrate northward consistently ~~northward migrated~~ in the direction of the modern northward-flowing south equatorial currents throughout their life span (Figs. 1~~–~~ and 2~~, and 3A)~~~~laterally migrated~~ ~~throughout their life span along their entire length (Gong et al., 2016)~~. It should be noted that ~~However, Lower Congo~~ channels on the West African slope with ~~in~~ water depth ~~of~~ > the effective depth of the south equatorial current~~s~~ do not have unidirectional migration trajectories (Ho et al., 2012).

ESTIMATING BANKFULL TURBIDITY CURRENT CONDITIONS FROM~~IN~~ DEEP-WATER ~~CHANNELS FROM~~ CHANNEL MORPHOLOGY

Unidirectionally Migrating Deep-Water Channels in the Lower Congo Basin

Six UCs of Quaternary age were recognized in the Lower Congo Basin (UC1 to UC6 in Fig~~s~~. ~~1–~~2). In cross-sectional view, they display asymmetrical channel cross-sections with northern channel flanks that are, overall, 1.5–3.5 times steeper than their southern counterparts (Fig. 2). They are composed of a series of seismically resolvable channel-complex sets that have bankfull channel widths of 1506–3817 m and bankfull channel depths of 64–108 m ~~(averaging 88 m)~~, giving aspect ratios of 16–45 ~~(averaging 28)~~ (Table DR1). In ~~plan view~~plan view, they are represented by alternating sets of closely spaced, crescent-shaped, straight, high- and low-amplitude threads (Fig. 3A), ~~display straight channel courses,~~ and have mean slope gradient (S) of 0.011–0.020 (averaging 0.015) ~~(dimensionless) (Fig. 3A)~~.

~~UC1 to UC6 consistently northward migrated in the direction of the modern northward-flowing south equatorial currents throughout their life span (Figs. 1, 2A, and 2B) along their entire length (Fig. 3A), forming some typical examples of channels with unidirectional trajectories. Deep-water channels are known as active conduits for turbidity currents (U_t in Figures 3B and 3C), while unidirectional channel migration represents the imprint of persistent contour currents (Gong et al., 2013, 2016; He et al., 2013~~**~~[[The in-text citation "He et al., 2013" is not in the reference list.]]~~**~~; Palermo et al., 2014~~**~~[[The in-text citation "Palermo et al., 2014" is not in the reference list.]]~~**~~). UCs, therefore, record the combined action of turbidity and contour currents.~~

Estimating Bankfull Turbidity Current Conditions ~~**in Deep-Water Channels**~~

~~Data on bankfull channel morphometrics as measured from the chosen channel cross-sections were used to compute bankfull turbidity current conditions, using the Froude number approach developed by Sequeiros (2012).~~ The Froude number method of Sequeiros (2012) returns ~~the normal density Froude number (~~ Fr~~) of turbidity currents~~ as a function of ~~average bed slope (SFr)~~, the combined friction factor for turbidity currents $[C_f(1+\alpha)]$, and the ratio of shear velocity to settling velocity (u_*/v_s), express as ~~(~~Equation 1~~)~~.

$$Fr = [0.15 + \tanh(7.62S^{0.75})](1 + v_s/u_*)^{1.1}[C_f(1+\alpha)]^{-0.21} \quad (1)$$

Publisher: GSA
Journal: GEOL: Geology
DOI:10.1130/G40204.1

It is applicable to both sinuous and straight deep-water channels (Sequeiros 2012), and was thus employed to estimate bankfull turbidity current conditions in ~~Lower Congo~~the studied UCs. Using Equation 1, Fr of turbidity currents in the studied channels was computed to range from 1.11 to 1.38 (averaging 1.24) (see the Data Repository for full details of our computation) ~~(see supplementary database for full details of our calculation processes)~~, thereby ~~exhibiting~~ displaying supercritical flow regimes (Fig. ~~DR1~~ 4A). ~~After the computations of Fr, t~~The layer-averaged velocity of channel turbidity currents (U_t) was then calculated via Equation 2.

$$U_t = Fr(g\overline{\Delta\rho}/\overline{\rho}h)^{1/2} \qquad (2)$$

where: (i) g is the gravitational acceleration; (ii) $\overline{\Delta\rho}$ refers to the layer-averaged excess density of the current; (iii) $\overline{\rho}$ denotes the layer-averaged density of the turbidity flow; and (iv) $\overline{\Delta\rho}/\overline{\rho}$ signifies the layer-averaged fractional excess density of the flow with respect to that of the ambient fluid (ρ_a) (i.e., $\overline{\Delta\rho}/\overline{\rho}$ of < 0.7% for field-scale turbidity currents, as suggested by Sequeiros, 2012). ~~Our results suggest that turbidity currents in the Lower Congo UCs had~~ U_t was then computed to range ~~of~~from ~1.72 to ~2.~~89~~ 859 m/s (Fig. ~~DR1~~ 4B; (see the Data Repository) ~~(Table DR1)~~. Cross-plot of our results of *S* and *Fr* against 73 measurements of *S* and *Fr* of turbidity currents has a high correlation coefficient ~~value~~ of R^2 = 0.82 (n = 82) (Fig. ~~DR1~~ 4A), validating the accuracy of our computations.

~~RESULTS:~~ HOW DO TURBIDITY FLOWS INTERACT WITH CONTOUR CURRENTS?

Parameterizing Amplitudes of Pycnoclines between Turbidity and Contour ~~Currents~~ Flows~~in Unidirectionally Migrating Deep-Water Channels~~

Wedderburn number (W) is widely used in ~~the~~ limnology research to estimate wind-forced internal seiche behaviors in lakes (Shintani et al., 2010), and is employed to ~~. The numerical approaches of a stratified lake to wind stress (i.e., W) are then used to~~ answer the question~~s~~ of how ~~do~~ turbidity flows interact with contour currents in Lower Congo UCs ~~(Figs. 4A and 4B**[[No figure matches the in-text citation "Figs. 4A and 4B". Please supply a figure and figure caption or delete the citation.]]**)~~? Tilting displacements of the interface between lower turbidity flows and upper contour currents (i.e., pycnoclines) would normally be parameterized by W:

$$W = \frac{g(\rho_2 - \rho_1)h^2}{\rho_1 v_*^2 B} = \frac{g(\Delta\rho)h^2}{\rho_1 v_*^2 B} \qquad (3)$$

where: (i) ρ_1 and ρ_2 are densities of upper contour currents and lower turbidity flows, respectively (Fig. ~~4A~~3B~~**[[No figure matches the in-text citation "Fig. 4A". Please supply a figure and figure caption or delete the citation.]]**~~); (ii) h denotes the thickness of the turbidity current; (iii) B is bankfull channel width (Fig. 3B~~4A**[[No figure matches the in-text citation "Fig. 4A".]]**~~); and (iv) v_* refers to to turbulent velocity at the interface between the water masses.

To compute W, four variables (ρ_2, $\Delta\rho$, B, and v_*) were~~need to be~~ determined. First, Sequeiros (2012) suggested that ~~the density of turbidity currents (ρ_2)~~ can be computed by:

$$\rho_2 = \rho_i(1 - C) + \rho_s C \qquad (4)$$

where ρ_i and ρ_s denote density~~ies~~ of the interstitial fluid and particles, respectively, and C signifies sediment concentration in~~of~~ the current. Assuming ρ_i = 1025 kg/m^3 and C = 1% being typical of turbidity currents, ρ_2 was then calculated to be 1041 kg/m^3.

~~where B_d is the bottom drag coefficient (B_d ≈0.001). Third,~~Second, ~~L~~ B was measured from nine chosen channel cross-sections (Table DR1). ~~Fourth~~Third, v_* is derived from the shear stress as $\tau = \rho_1 v_*^2 = \rho_1 C_d U_c{}^2$ (Shintani et al., 2010), so that:

$$v_* = \sqrt{C_d} U_c$$ (~~7~~5)

where: (i) C_d is the drag coefficient, and is set by the interfacial environment rate ~~(i.e., the mixing turbulence between the turbidity currents and the stagnant ambient fluid)~~ and (ii) U_c~~U_c~~ is the velocity of the contour currents. ~~Paleocurrent velocities of the south equatorial currents ($U_c$$U_c$) involved in the construction of the documented UCs are~~ is poorly constrained ~~(Mercier et al., 2003)~~; however, existing data sets suggest that ~~the mean velocities of contour currents are~~it is in many cases between ~~10~~0.10–0.30 ~~c~~ m/s (Wetzel et al., 2008). W ~~of pycnoclines between turbidity and contour currents in Lower Congo UCs~~ was~~,~~ then~~,~~ computed to range from 0.21 to 1.04 ~~(averaging 0.65)~~ (when U_c~~U_c~~ = 0.10 ~~10 c~~m/s) or to vary from 0.07 to 0.35 ~~(averaging 0.22)~~ (when U_c~~U_c~~ = ~~30 cm/s~~0.30 m/s) (Fig. ~~DR1~~ 4C).

Shintani et al. (2010) have suggested that ~~The slope of the density interface is estimated to be equal to −1/Ri where Ri is the Richardson number, and is defined as $Ri = g'h_1/v_*^2$, with h_1 being the upper layer thickness at the rest condition (Shintani et al., 2010). Therefore,~~ the amplitude of the deflections of pycnoclines ~~between~~

DOI:10.1130/G40204.1

~~turbidity and contour currents in the studied channels~~ (A) can be estimated by ~~Equation 8~~:

$$A = \frac{L}{2h_1 Ri} = \frac{1}{2W}. \qquad (~~8~~6)$$

Our results suggest that A ranges from 0.48 to 2.36 m, when U_c ~~U_e~~ = ~~10 cm/s~~0.10 m/s; or ~~that that A varies~~ from 1.44 to7.07 m, when U_c ~~U_e~~ = ~~30 cm/s~~0.30 m/s (Fig. 4C) ~~(Table DR1)~~.

Parameterizing the Internal Wave Field Along ~~the~~ Pycnoclines ~~between Turbidity and Contour Currents in Unidirectionally Migrating Deep-Water Channels~~

The internal pycnocline response of turbidity flows in the studied channels to a forcing event of contour currents can be gauged by the new Wedderburn number (W^{-1}) (Boegman et al., 2005), defined as:

$$W^{-1} = \frac{A \eta_0}{h_1^`} \qquad (~~9~~7)$$

where: ~~η_0 and~~ $h_1^`$ is~~are~~ the ~~maximum interference displacement and the~~ interface depth~~, respectively~~. W^{-1} was estimated to range from 0.96 to 4.71, when U_c ~~U_e~~ = ~~10 cm/s~~0.10 m/s; or from 2.87 to 14.13, when U_c ~~U_e~~ = ~~30 cm/s~~0.30 m/s. Boegman et al. (2005) have suggested that strong forcing (represented by $0.96 < W^{-1}$) would most likely produce Kelvin-Helmholtz (K-H) billows and bores.

Reconstructing K-H Billows ~~and Bores~~ or Bores Along Pycnoclines

Supercritical turbidity currents in the studied UCs are typically ~~of the~~ stratified flows, and thus have their peak velocit~~yies computed as 21.2572–32.51 89 m/s~~ near the bed ~~(Table DR1)~~. A representative velocity at the interface of such stratified

Publisher: GSA
Journal: GEOL: Geology
DOI:10.1130/G40204.1

supercritical flows would, thus, be lower than their layer-averaged or peak velocity~~ (Sequeiros et al., 2010)~~. ~~A representative velocity at the interface between turbidity and contour currents~~ The representative velocity at the interface ~~–~~is poorly constrained, but can be ~~is, therefore,~~ assumed to be $U_t/2$ for maximum (Dr. Octavio E. Sequeiros, pers. comm. 2017). The local paleocurrent velocities (v) and directions (β) of K-H billows and bores ~~and bores~~ were computed by Equation ~~10~~ 8 and Equation ~~11~~9, respectively (Fig. ~~DR1~~ 3B):

~~V~~ $$v = \sqrt{(\frac{U_t}{2})^2 + U_c^2}$$ (~~Equation 10~~8)

$$\beta = \arctan[U_c/(\frac{U_t}{2})].$$ (~~Equation 11~~9)

Our results suggest that when U_c ~~U_c~~ = ~~10 cm/s~~0.10 m/s, v and β ~~of K-H billows and bores in the studied channels~~ were computed to range from 0.87 to 1.~~45~~ 45 m/s and 4.0° to 6.6°, respectively (Fig. ~~DR1~~ 4D); or that when U_c ~~U_c~~ = ~~30 cm/s~~0.30 m/s, v and β were calculated to range from ~~of~~ 0.91 to –1.48 m/s and 11.7° to 19.2°, respectively (Fig. ~~DR1~~ 4D).

~~DISCUSSION:~~ HOW DOES THE INTERPLAY OF TURBIDITY AND CONTOUR CURRENTS DETERMINE SEDIMENTATION?

As discussed above, the interplay of turbidity and contour currents in the studied UCs would have produced pycnoclines that had A of 0.48–7.07 m~~ (averaging 2.04 m)~~, and likely ~~was found to~~ yielded K-H billows and bores, which propagated toward and impinged the~~toward northern steep flanks~~steep channel flanks by 4.0° to 19.2°. They therefore~~, thus,~~ generated~~had~~ the strongest shocks, largest amplitudes, and longest wavelengths at their fronts along the ~~northern steep flanks~~steep flank of any

DOI:10.1130/G40204.1

channels. Conversely, the weakest shocks, shallowest oscillations, smallest amplitudes, and shortest wavelengths are expected at their rears along the southern gentle flanksgentle flanks (Figs. 3B and 3CFigs. 4A and 4B**[[No figure matches the in-text citation "Figs. 4A and 4B".]]**). The steep channel flanks frequently impinged by wavefronts, thus, were thus more prone too become erosionded by turbulent mixing between turbidity and contour currents.

The suggestedabove flow structures of K-H billows and bores with wave fronts along the steep channel flanks versus wave tails along the gentle channel flanks isare supported by the following three lines of evidence (Figss. 3B and 3C). First, the Lower Congo UCs display asymmetrical channel cross-sections with northern steep flankssteep flanks that are, overall, 1.5–3.5 times steeper than their southern gentle flanks (Figs. 2 and 3A). Second, high-amplitude seismic reflections suggestive sandsier preferentially accumulated along the northern steep flankssteep flanks, whereas low-amplitude seismic reflections indicative of muddier deposits preferentially accumulated along gentle flanks (Fig. 3A2). Third, steep flanks contain truncation terminations, whereas their gentle flanks exhibit downlap terminations (Fig. 3A 3B2B). All of these observations collectively point to steep-flank erosion versus gentle-flank deposition, suggesting the occurrence of wavefronts along the steep flanks versus wavetails along gentle flanks (Figs. 4A 3B and 4B3C**[[No figure matches the in-text citation "Figs. 4A and 4B".]]**). Contour currents generally display predominantly unidirectional flow conditions (Wetzel et al., 2008), suggesting that K-H billows and bores would have persistently promoted steep-flank erosion

Publisher: GSA
Journal: GEOL: Geology
DOI:10.1130/G40204.1

versus gentle-flank deposition, forcing individual channels to consistently migrate in the direction of the~~toward~~ ~~northern steep flanks~~steep flanks through time (Fig~~s~~. 2, 3B~~-~~, and 3C~~A~~).

CONCEPTUAL IMPLICATIONS

Our results provide~~have~~ three main~~ conceptual~~ contributions towards better understanding of unidirectionally migrating deepwater channels. Firstly, UCs were recently recognized on the northern South China Sea margin (Gong et al., 2013~~; He et al., 2013~~**~~[[The in-text citation "He et al., 2013" is not in the reference list.]]~~**), and were also well developed in the Lower Congo Basin (Fig~~s~~. 2~~ and 3A~~) and offshore Northern Mozambique (Palermo et al., 2014**~~[[The in-text citation "Palermo et al., 2014" is not in the reference list.]]~~**). They are, thus, fairly common on continental margins~~ worldwide~~, although they are quite~~dramatically~~ different from well-documented turbidite or contourite channels. This study succeeds in using W to interpret unidirectional along-slope channel migration, and quantifies the pycnocline response of turbidity flows to the forcing of contour currents for the first time, thereby contributing to a more complete picture of flow processes and sedimentation in submarine channels.

Secondly, the general energy differences between turbidity and contour currents have mad~~k~~e their interaction one of the most controversial issues since the 1970s (e.g., Rebesco et al., 2014). Our results suggest that, in most cases, pycnoclines between turbidity and contour currents could produce K-H billows and bores that impinged the~~toward~~ steep channel flanks (Figs. ~~4A~~ 3B and ~~4B~~3C**~~[[No figure matches~~**

Publisher: GSA
Journal: GEOL: Geology
DOI:10.1130/G40204.1

~~**the in-text citation "Figs. 4A and 4B".]]**~~). Their shocking wave fronts ~~with the strongest shocks~~ and deep~~est~~ oscillations ~~were more prone to~~ promoted steep-flank erosion, whereas their wavetails ~~with the weakest shocks~~ with~~and~~ shallow~~est~~ oscillations would have~~are more prone to~~ promoted gentle-flank deposition. Our results, therefore, help to better understand and provide a new model of the interplay of turbidity and contour currents~~, which are completely new and different from the current turbidite or contourite facies model~~. Our results, therefore, may set the tone in exploring further quantification~~s~~ of the interplay of ~~the~~ oceanic~~ography of~~ contour currents and the sedimentology of turbidity currents.

Thirdly, it is now widely acknowledged that turbidity currents carry~~are carrying~~ a significant sedimentary load, ~~and~~ are brief events~~short~~ (a few days per year), local and intense, and draw~~ing mainly~~ the attention of mainly sedimentologists (~~Peakall and Sumner 2015;~~ Azpiroz-Zabala et al., 2017). Conversely, contour currents are essentially clean-water~~s~~, ~~and are~~ long-lived (up to millions of years), of great~~large~~ spatial extent, and have the attention~~mild, drawing~~ mainly ~~the attention~~ of oceanographers (Rebesco et al., 2014). Therefore, turbidity and contour currents are usually not addressed jointly. However, our observations have shown that the depositional/erosional record of some deep-water~~turbidite~~ channels ~~may~~ contain clear signals~~carry a considerable imprint~~ from both turbidity and contour currents, and we advocate closer collaboration between~~highlighting that~~ stratigraphic communities that separately ~~analysis~~ analyze turbidity or contour currents ~~should more closely collaborate~~.

Publisher: GSA
Journal: GEOL: Geology
DOI:10.1130/G40204.1

CONCLUSIONS

We used the concept of~~ ?~~ Wedderburn Number~~ *W*~~, for the first time, to quantify pycnocline response of turbidity currents to forcing events of contour currents in widely occurring UCs. Pycnoclines between turbidity and contour currents would be~~have~~ produced~~,~~ when contour currents with boundary current velocities (assumed constant between ~~10 and 30 cm/s~~0.10 and 0.30 m/s) flowed across the pathway of supercritical turbidity flows in submarine channels~~ turbidity flows~~ with Fr of 1.11–1.38 and U_t of 1.72–2.~~89~~ 59 m/s. They had *W* of 0.07–1.04 and *A* of up to 7.07 m, and would thus, in most case, have produced K-H billows and bores. These K-H billows and bores had velocities of 0.87–1.48 m/s and impinged toward the steep flanks by 4.0° to 19.2°. Therefore, their wavefronts with the strongest shocks and deepest oscillations~~,~~ would have occurred preferentially~~ occur~~ along the steep channel flanks,~~ and~~ constantly promoting~~ed steep-flank~~ erosion and resultant steep channel walls with common~~widespread~~ occurrence of truncation terminations. Their wavetails with the weakest shocks and shallowest oscillations, in contrast, would have occurred preferentially~~ occur~~ along the gentle channel flanks,~~ and consistently~~ favoring~~ed~~ gentle-flank deposition~~, and resultant~~ and gentle channel walls with widespread ~~occurrence of~~ downlap stratal terminations. Such asymmetric intra-channel deposition would have persistently forced individual channels to migrate in the direction of~~toward~~ the steep flanks through time, as recorded by unidirectional channel-growth trajectories.

ACKNOWLEDGMENTS

This research was jointly funded by the Independent Project of State Key Laboratory of Petroleum Resources and Prospecting (No. PRP/indep-1-1701) and the Science Foundation of China University of Petroleum, Beijing (No. 2462017YJRC061) ~~and the Independent Project of State Key Laboratory of Petroleum Resources and Prospecting (No. PRP/indep-1-1701)~~ to C Gong~~by the Science Foundation of China University of Petroleum, Beijing (No. 2462017YJRC061) to C. Gong~~ and by the National Natural Science Foundation of China (No. 41372115) to Y Wang. This study has been significantly improved by comments from journal editor James Schmitt and reviewers of Joris Eggenhuisen and Octavio E. Sequeiros.

REFERENCES CITED

Azpiroz-Zabala, M., Cartigny, M.J., Talling, P.J., Parsons, D.R., Sumner, E.J., Clare, M.A., Simmons, S.M., Cooper, C., and Pope, E.L., 2017, Newly recognized turbidity current structure can explain prolonged flushing of submarine canyons, Science advances, 3:~~,~~ e1700200.

Boegman, L., Ivey, G.N., and Imberger, J., 2005, The degeneration of internal waves in lakes with sloping topography: Limnology and Oceanography, v~~-~~. 50, p~~-~~. 1620–1637, https://doi.org/10.4319/lo.2005.50.5.1620.

de Leeuw, J., Eggenhuisen, J.T., and Cartigny, M.J.B., 2016, Morphodynamics of submarine channel inception revealed by new experimental approach: Nature Communications, v. 7, p. 10886, https://doi.org/10.1038/ncomms10886.

Gong, C., Wang, Y., Zhu, W., Li, W., and Xu, Q., 2013, Upper Miocene to Quaternary unidirectionally migrating deep-water channels in the Pearl River

Mouth Basin, northern South China Sea: The American Association of Petroleum Geologists Bulletin, v–. 97, p–. 285–308, https://doi.org/10.1306/07121211159.

Ho, S., Cartwright, J.A., and Imbert, P., 2012, Vertical evolution of fluid venting structures in relation to gas flux, in the Neogene-Quaternary of the Lower Congo Basin, Offshore Angola: Marine Geology, v. 332–334, p. 40–55, https://doi.org/10.1016/j.margeo.2012.08.011.

Mercier, H., Arhana, M., and Lutjeharms, J.R.E., 2003, Upper-layer circulation in the eastern Equatorial and South Atlantic Ocean in January-March 1995: Deep-sea Research. Part I, Oceanographic Research Papers, v. 50, p. 863–887, https://doi.org/10.1016/S0967-0637(03)00071-2.

Palermo, D., Galbiati, M., Famiglietti, M., Marchesini, M., Mezzapesa, D., and Fonnesu, F., 2014, Insights into a new super-giant gas field - sedimentology and reservoir modeling of the coral complex, offshore northern Mozambique. OTC-24907-MS.

Parsons, D.R., Peakall, J., Aksu, A.E., Flood, R.D., Hiscott, R.N., Besiktepe, S., and Mouland, D., 2010, Gravity-driven flow in a submarine channel bend: Direct field evidence of helical flow reversal: Geology, v. 38, p. 1063–1066, https://doi.org/10.1130/G31121.1.

Peakall, J., and Sumner, E.J., 2015, Submarine channel flow processes and deposits: A process-product perspective: Geomorphology, v. 244, p. 95–120, https://doi.org/10.1016/j.geomorph.2015.03.005.

Publisher: GSA
Journal: GEOL: Geology
DOI:10.1130/G40204.1

Pyles, D.R., Tomasso, M., and Jennette, D.C., 2012, Flow processes and sedimentation associated with erosion and filling of sinuous submarine channels: Geology, v. 40, p. 143–146, https://doi.org/10.1130/G32740.1.

Rebesco, M., Hernández-Molina, F.J., Rooij, D.V., and Wåhlin, A., 2014, Contourites and associated sediments controlled by deep-water circulation processes: State-of-the-art and future considerations: Marine Geology, v. 352, p. 111–154, https://doi.org/10.1016/j.margeo.2014.03.011.

Shintani, T., de la Fuente, A., Niño, Y., and Imberger, J., 2010, Generalizations of the Wedderburn number: Parameterizing upwelling in stratified lakes: Limnology and Oceanography, v. 55, p. 1377–1389, https://doi.org/10.4319/lo.2010.55.3.1377.

Sequeiros, O.E., 2012, Estimating turbidity current conditions from channel morphology: A Froude number approach: Journal of Geophysical Research, v. 117, C04003, https://doi.org/10.1029/2011JC007201.

Sequeiros, O.E., Spinewine, B., Beaubouef, R.T., Sun, T., Garaía, M.H., and Parker, G., 2010, Characteristics of velocity and excess density profiles of saline underflows and turbidity currents flowing over a mobile bed: Journal of Hydraulic Engineering, v. 136, p. 412–433, https://doi.org/10.1061/(ASCE)HY.1943-7900.0000200.

Stramma, L., and England, M., 1999, On the water masses and mean circulation of the South Atlantic Ocean: Journal of Geophysical Research. Oceans, v. 104, p. 20863–20883, https://doi.org/10.1029/1999JC900139.

Wetzel, A., Werner, F., and Stow, D.A.V., 2008, Bioturbation and biogenic sedimentary structures in contourites, *in* Rebesco, M., and Camerlenghi, A., eds., Contourites: Developments in Sedimentology: Oxford, UK, Elsevier, v. 60, p. 183–202, https://doi.org/10.1016/S0070-4571(08)10011-5.

FIGURE CAPTIONS

Figure 1. Google Earth image showing geographical and oceanographic context of the study area in the Lower Congo Basin.

Figure 2. (A) Strike-view seismic section showing cross-sectional seismic expression of six UCs. (B) Strike-oriented seismic line (line locations shown in Fig. 3A) showing a close-up view of Lower Congo UC1 to UC3.

Figure 3. (A) Representative time slice taken 350 ms below the modern seafloor showing plan-view geomorphological expression of UC1 to UC3. (B and C) Schematic illustrations of a simple two-layer model employed to quantify how turbidity and contour currents act together and jointly determined sedimentation in UCs.

Figure 4. Scatterplots of S ~~vs.~~versus Fr (A), U_t versus ~~vs.~~ z_p/h (B), W against A (C), and *ß* against *V* (D).

1GSA Data Repository item 2018xxx, xxxxxxxx, is available online at http://www.geosociety.org/datarepository/2018/ or on request from editing@geosociety.org.

Figure

Click here to download Figure Figure 1.tif

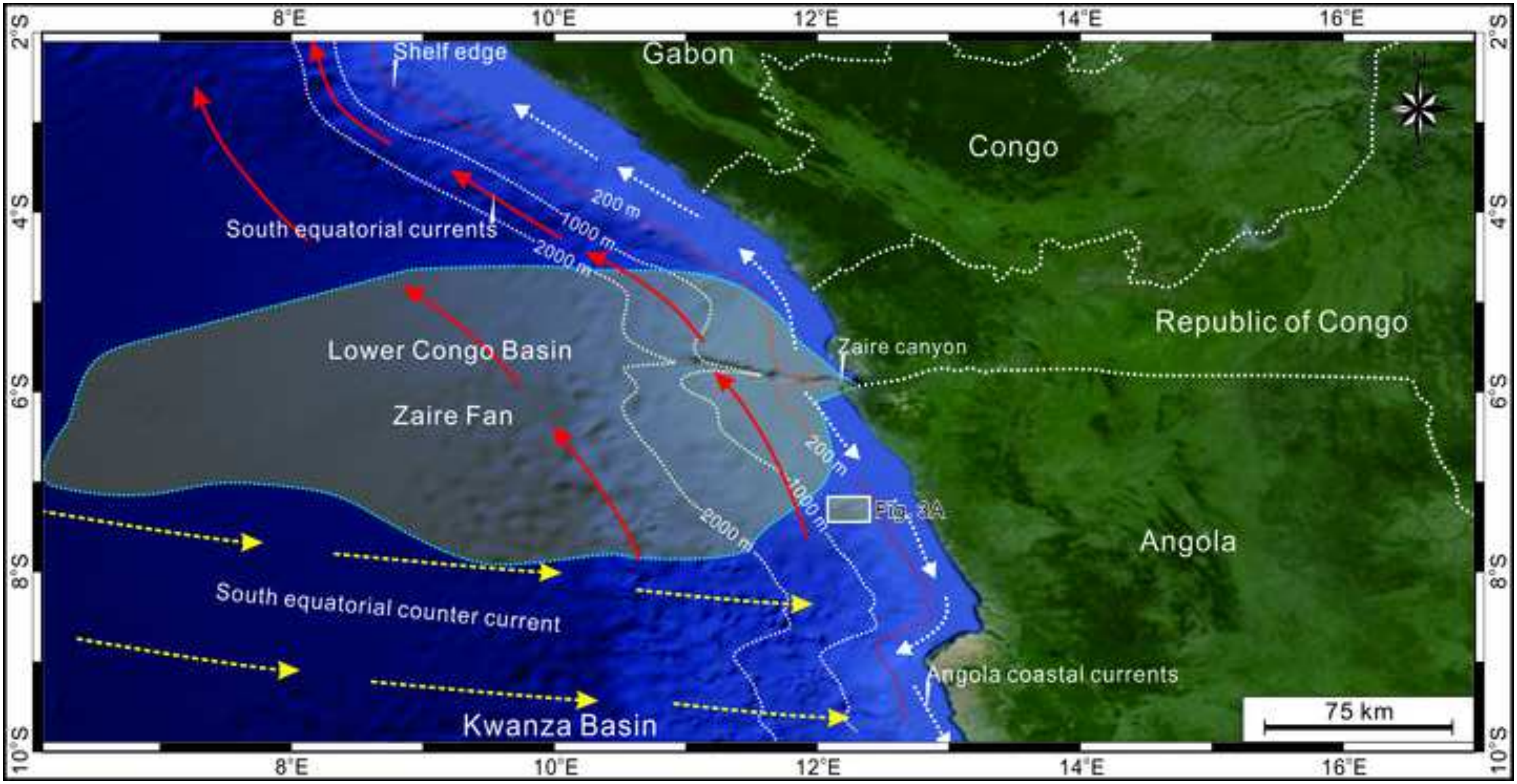

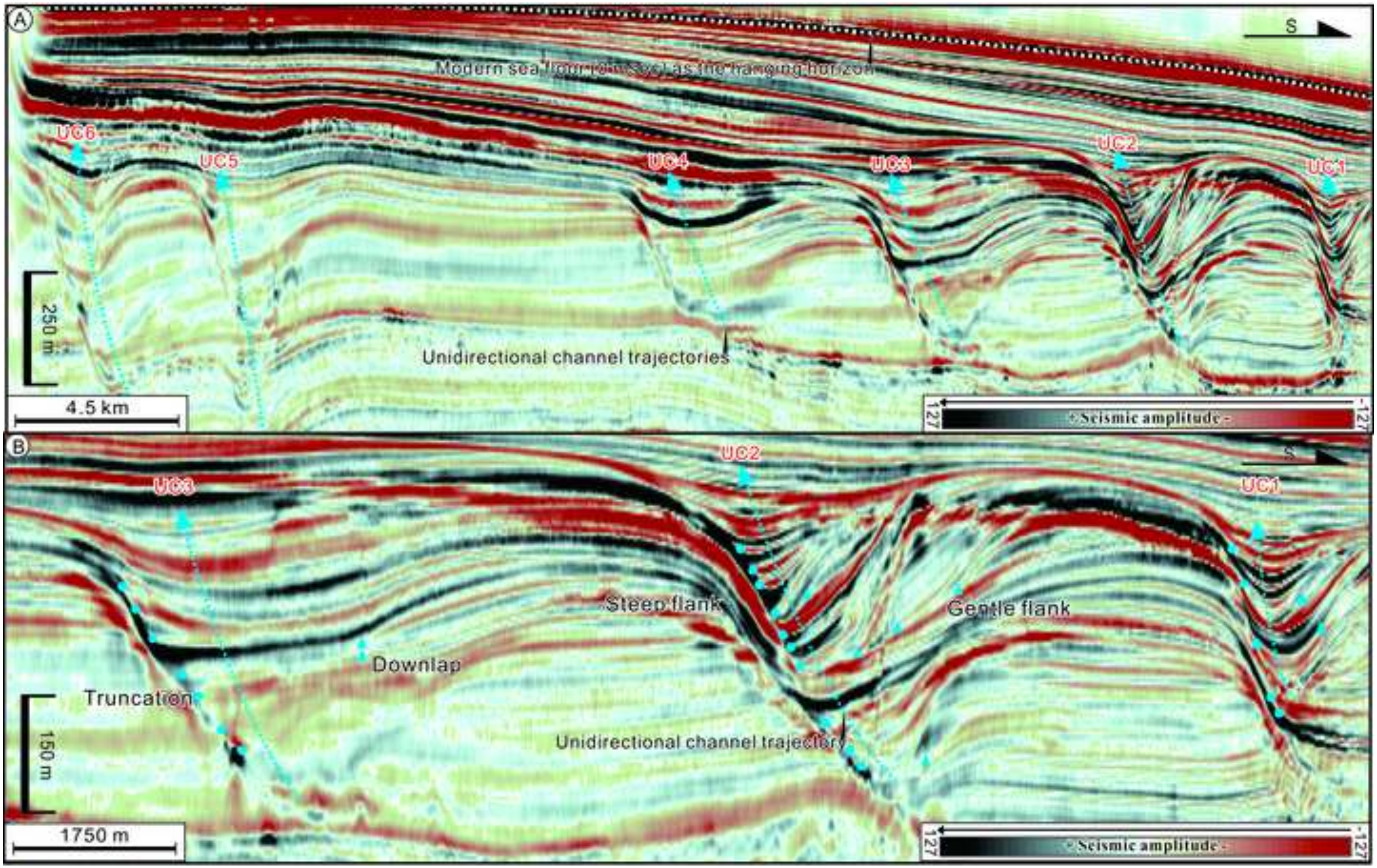
A
S
Modern sea floor (or T0) as the hanging horizon
UC6
UC5
UC4
UC3
UC2
UC1
250 m
Unidirectional channel trajectories
4.5 km
127
Seismic amplitude
-127
B
S
UC3
UC2
UC1
Steep flank
Gentle flank
Downlap
Truncation
150 m
Unidirectional channel trajectory
1750 m
127
Seismic amplitude
-127

Figure

Click here to download Figure Figure 3.tif

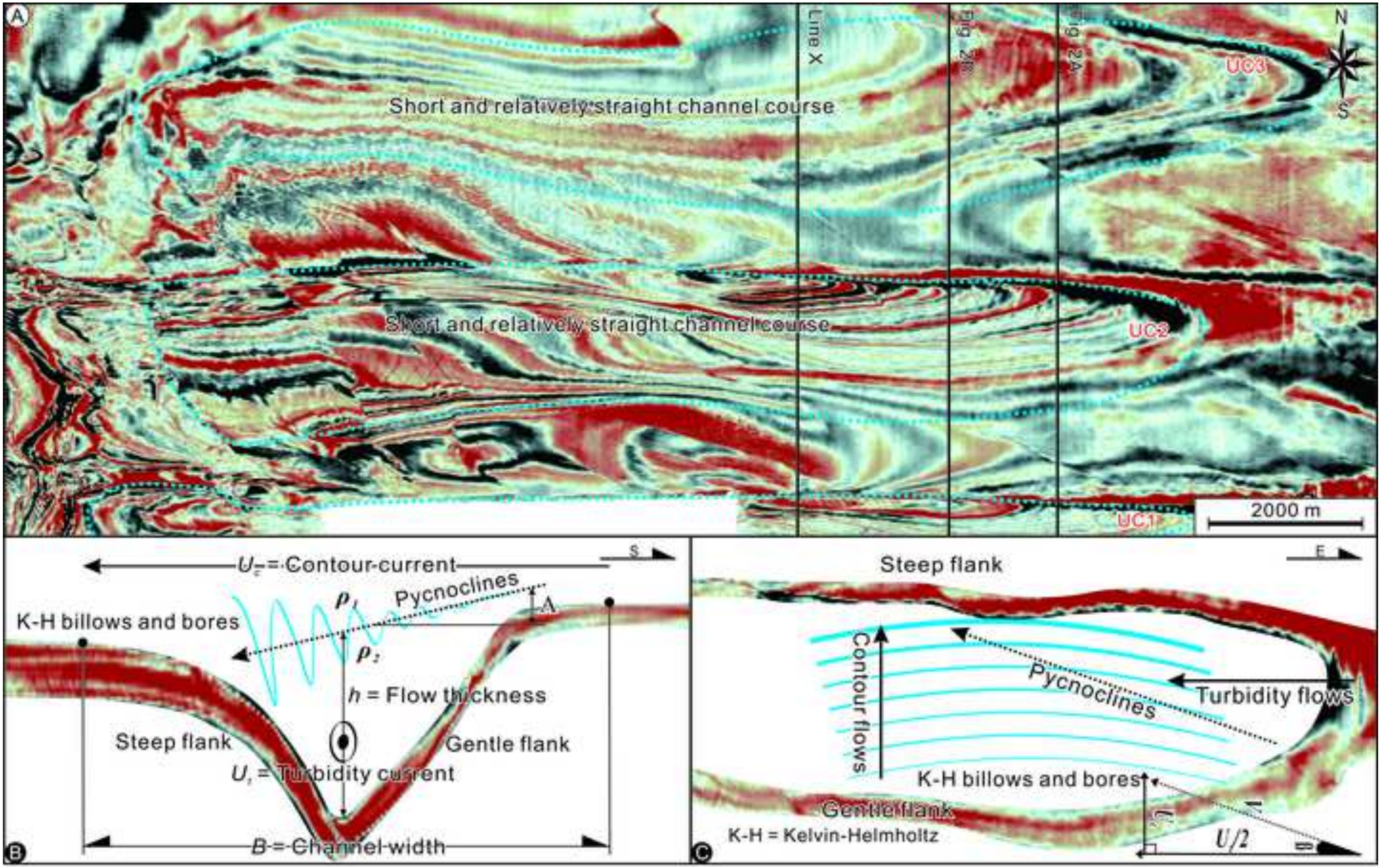

Figure

Click here to download Figure Figure 4.tif

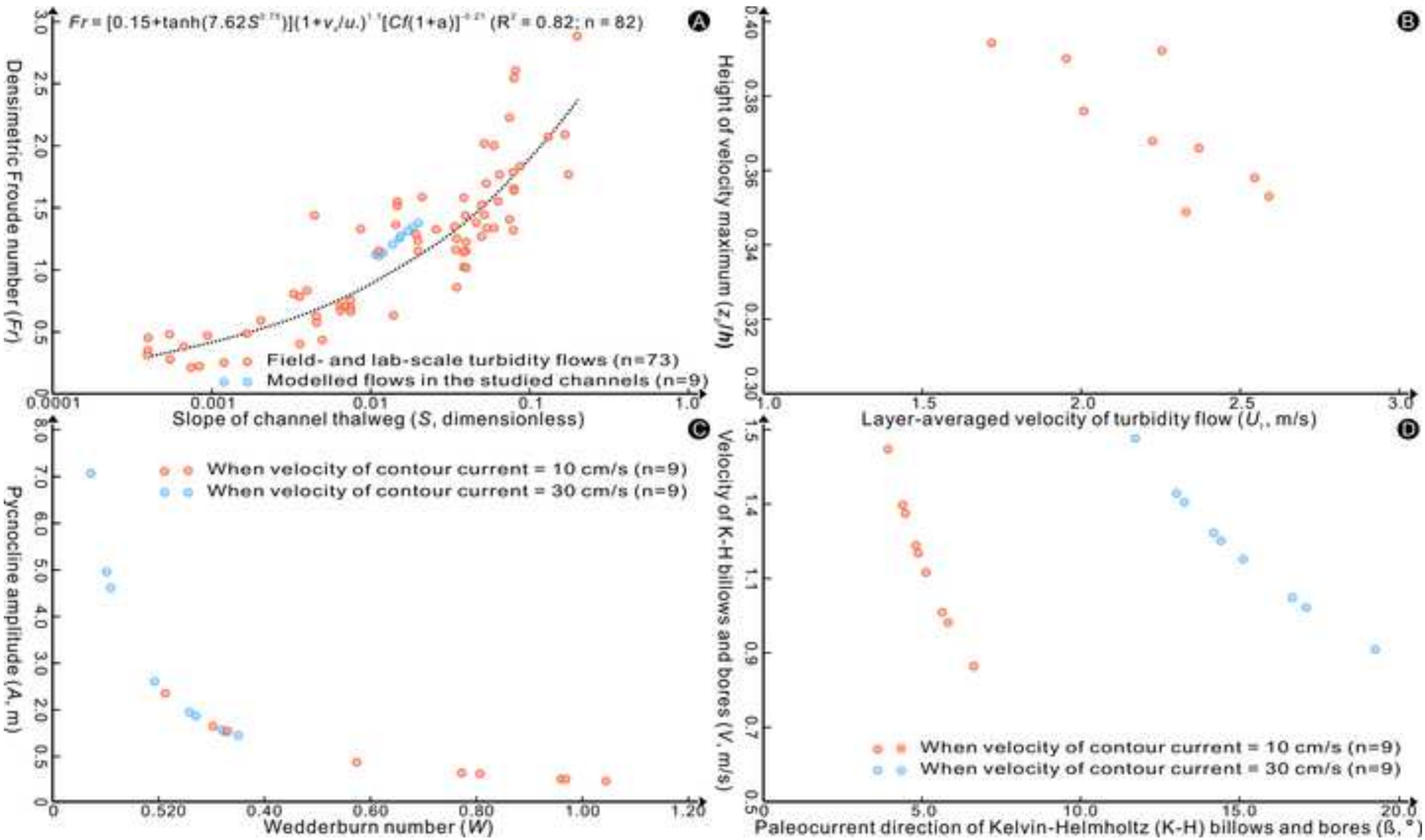

3D SEISMIC DATABASE AND METHODOLOGY

Quantification of channel morphology and architecture

The primary source of the database utilized in the current study is ca 500 km^2 km^2 of 3D seismic data, acquired by the China Petroleum and Chemical Corporation from the Lower Congo Basin, West African margin (Fig. 1). 3D seismic data have been migrated with a single pass 3D post-stack time migration, and have a bin size spacing of 12.5 m (in-line) by 12.5 m (cross-line) and a sampling interval of 4 ms. The frequency of the time-migrated volume varies with depth, but is approximately 50 Hz for the study interval of interest, yielding a vertical (λ/4) resolution of 7.5 m and a detection of 1.2 m (λ/25). They were displayed using "SEG (Society of Exploration Geophysics) reverse polarity", where a positive reflection coefficient corresponds to an increase in acoustic impedance, and is represented by a positive reflection event. They were displayed using a red-white-black color bar, on which a peak (a decrease in acoustic impedance) is represented by the black and a trough (an increase in acoustic impedance) is represented by the red.

3D seismic data were used to quantify morphologies and architecture of the studied channels, using "traditional" 2D stratigraphic analyses and 3D geomorphological approaches. The flattened horizontal seismic amplitude slices were produced by the Lower Congo 3D seismic volume flattened by the present-day seafloor (0 msec). Flattened horizontal seismic amplitude slices, together with with 2D seismic transects, were then used to delineate both plan-view and cross-sectional seismic manifestations of unidirectionally migrating deep-water channels as documented in this study. Our measurements of the morphometric properties of the studied channels were converted from time to depth, using an average velocity of 1500 m/s for seawater and 2003 m/s for the shallow siliciclastics (Gong et al., 2016).

Estimating bankfull turbidity current conditions from channel morphology

The Froude number approach developed by Sequeiros (2012) is applicable for both straight and sinuous deep-water channels, and is, thus, employed to estimate bankfull turbidity current conditions in the studied UCs (UC1 to UC3 on Figs. 2 and 3A). The predictive equation (Eq. 1) of this method returns the densimetric Froude number (Fr) of turbidity current as a function of: (i) the average bed slope (S); (ii) the combined friction factor $[C_f(1+\alpha)]$; and (iii) the ratio between the settling velocity of the suspended sediment (v_s) and the shear velocity of the current (u_*) (Sequeiros, 2012). Because $[C_f(1+\alpha)]$ depends on flow conditions as represented by Fr, the Froude number approach requires iteration. Six complementary equations (Eq. 2 to Eq. 7) were, thus, proposed to relate other key flow parameters to Fr.

$$Fr = [0.15 + \tanh(7.62S^{0.75})](1 + v_s/u_*)^{1.1}[C_f(1+\alpha)]^{-0.21} \qquad \text{(Eq. 1)}$$

$$\alpha = 0.15Fr^{3.95} \qquad \text{(Eq. 2)} \qquad \frac{z_p}{h} = 0.42Fr^{-0.58} \qquad \text{(Eq. 3)}$$

$$\frac{u_p}{U_t} = 1.15 + 0.14Fr^{1.30} \qquad \text{(Eq. 4)} \qquad \frac{z_c}{h} = 0.09Fr^{-2.80} \qquad \text{(Eq. 5)}$$

$$\frac{c_c}{C} = 1.15 + 0.20Fr^{2.90} \qquad \text{(Eq. 6)} \qquad \frac{h}{z_i} = 0.78Fr^{-0.21} \qquad \text{(Eq. 7)}$$

where (i) z_p is the height of the maximum velocity point above the bottom; (ii) h and U_t are layer-averaged thickness and velocity of the turbidity current, respectively; (iii) u_p is the peak velocity; (iv) c_c and C denotes the maximum concentration and layer-averaged suspended sediment concentration, respectively; and (v) z_i signifies the distance from the channel bed to the interface between the current and ambient water. Eq. 1 to Eq. 7, together with the bed resistance relation for channel turbidity currents (Cz_p) (Eq. 8) and an equation for friction coefficient (Eq. 9), allow closing the loop of Eq. 1 to Eq. 9.

$$Cz_p = u_p/u_* = 1/\kappa\ln(30z_p/k_s) \qquad \text{(Eq. 8)}$$

$$\mathrm{C_f} = (u_*/U_t)^2 \qquad \text{(Eq. 9)}$$

where: (i) κ is the von Karman constant, and is equal to 0.405; (ii) k_s refers to the bed roughness height; and (iii) C_f denotes friction coefficient.

To compute Fr, seven variables (i.e., C, $\overline{\Delta\rho}/\overline{\rho}$, u_*/v_s, C_f (1+α), S, z_i and κ_s) need to be estimated. Firstly, turbidity currents are diluted flows with siliciclastic material, and generally have the layer-averaged volumetric concentration (C) of < 5% (Sequeiros, 2012). Secondly, a review and systematic analysis of 78 published works containing 1092 estimates of velocity and concentration of gravity flows from both field measurements and laboratory experiments dating as far back as the early 1950s suggests that the mean range of layer-averaged fractional excess density of turbidity flows ($\overline{\Delta\rho}/\overline{\rho}$) varies from 0.4% to 0.7% (0.25% < C < 0.45% with ρ_s = 2650 kg/m^3) (Sequeiros, 2012). Thirdly, laboratory experiments suggest that u_*/v_s varies from 5 to 50. Fourthly, previous studies suggest that laboratory-scale turbidity currents have C_f (1+α) of 0.01 to 0.07, and that field-scale turbidity flows have C_f (1+α) of 0.001 to 0.01. Fifthly, S and z_i were estimated from nine chosen channel cross-sections (UC1 to UC3 in Figs. 2 and on seismic line X on Fig. 3A), which have S of 0.011 to 0.020 (averaging 0.015) (Table DR1). z_i was assumed to be equal to bankfull depths of individual channel-complex sets (reported as H of 64 to 108 m, with mean value of H = 88 m). Sequeiros (2012) suggested that turbidity currents with relatively coarse suspended materials have κ_s of 0.01 to 1 m.

To start iterating, we assumed an arbitrary Fr to calculate α, C_f and other secondary variables. α was firstly calculated via Eq. 2, while Cz_p, z_p, and h were then computed by Eq. 8, Eq. 3, and Eq. 7, respectively. A bed resistance relation for turbidity flows (Eq. 10) was introduced to compute C_f.

$$\mathrm{C_f} = \left(\frac{u_*}{U_t}\right)^2 = \left(\frac{u_p}{Cz_p \times U_t}\right)^2 \qquad \text{(Eq. 10)}$$

where: (i) u_p/U_t and Cz_p come from Eq. 4 and Eq. 8, respectively. After such iterative processes, the loop of Eq. 1 to Eq. 9 was finally closed, resulting in values of Fr, α, h, z_p, Cz_p, u_p/U_t, and C_f as listed in Table DR1. Fr of turbidity currents in the studied channels was computed to range from 1.11 to 1.38 (averaging 1.24), thereby exhibiting supercritical flow regimes (Table DR1). After the computations of Fr, the layer-averaged velocity (U_t) was then calculated via Eq. 11.

$$U_t = Fr(g\overline{\Delta\rho}/\overline{\rho}h)^{1/2} \qquad \text{(Eq. 11)}$$

where: (i) g is the gravitational acceleration; (ii) $\overline{\Delta\rho}$ refers to the layer-averaged excess density of the current; (iii) $\overline{\rho}$ denotes the layer-averaged density of the turbidity flow; and (iv) $\overline{\Delta\rho}/\overline{\rho}$ signifies the layer-averaged fractional excess density of the flow with respect to that of the ambient fluid (ρ_a) (i.e., $\overline{\Delta\rho}/\overline{\rho}$ of < 0.7% for field-scale turbidity currents, as suggested by Sequeiros, 2012). Our results suggest that turbidity currents in the Lower Congo UCs had U_t of 1.72 to 2.59 m/s (averaging 2.22 m/s) and low heights of velocity maximum (i.e. 0.35 to 0.39 of the flow height) (Table DR1).

Our results of *S* and *Fr* were, then, plotted together with 73 measurements of *S* and *Fr* of field- and laboratory-scale turbidity current (Sequeiros, 2012), resulting in a power law relationship of *Fr* to *S* (R^2 = 0.84; n=82) (Table DR1). Given geological and methodological uncertainties, the agreement between *Fr* as iteratively calculated via Eq. 1 to Eq. 10 and those in published source articles is surprisingly good, validating the accuracy of our computations.

In addition, a direct comparison between our results and measurements of 30 field-scale and 43 laboratory-scale submarine channel turbidity currents was conducted (Sequeiros 2012), in order to validate the accuracy of our computations. After the determination of turbidity current conditions in the studied channels, model of a stratified lake to wind stress and associated concept of Wedderburn number (*W*) and new Wedderburn number (W^{-1}) are used to answer the questions of how do turbidity flows interact with contour currents in unidirectionally migrating deep-water channels recognized in the Lower Cogon Basin (Stevens and Lawrence, 1997; Boegman et al., 2005).

REFERENCES

Boegman, L., Ivey, G.N., and Imberger, J., 2005. The degeneration of internal waves in lakes with sloping topography: Limnology and Oceanography, v. 50, p. 1620–1637.

Gong, C., Wang, Y., Steel, R., Peakall, J., Zhao, X., and Sun, Q., 2016, Flow processes and sedimentation in unidirectionally migrating deep-water channels: From a three-dimensional seismic perspective: Sedimentology, v. 64, p. 233–249.

Sequeiros, O.E., 2012, Estimating turbidity current conditions from channel morphology: A Froude number approach: Journal of Geophysical Research, v. 117 C04003.

Stevens, C.L., and Lawrence, G.A., 1997, Estimation of wind-forced internal seiche amplitudes in lakes and reservoirs, with data from British Columbia, Canada: Aquatic Sciences, v. 59, p. 115–134.

Table DR1. Tabulation of bankfull turbidity current conditions and parameters used to quantify the internal wave field along pycnoclines between turbidity and contour currents. Please refer to notation section for full details of parameters listed in this table.

Seismic lines	Channels	Estimating bankfull turbidity currents from channel morphology												Parameterizing internal wave field along pycnoclines between turbidity and contour currents															
		Input				Iterate	Output				C	Output		Input						Output									
		S	z_i	κ_s	v_s/u_*	Fr	α	C_f	h	z_p		U_t	U_p	g	ρ_2	C_d	U_{c1}	U_{c2}	B	W (-)		A (m)		W^{-1} (-)		v (m/s)		ß (º)	
		-	m	m	-	-	-	-	m	m	-	m/s	m/s	m/s^2	kg/m^3	-	m/s	m/s	m	U_{c1}	U_{c2}	U_{c1}	U_{c2}	U_{c1}	U_{c2}	U_{c1}	U_{c2}	U_{c1}	U_{c2}
Figure 2A	UC1	0.020	80	1	0.002	1.38	0.531	0.0074	58.3	20.4	0.0032	2.33	3.16	9.80	1041	0.01	0.1	0.3	1612	0.77	0.26	0.65	1.94	1.30	3.89	1.17	1.20	4.9	14.4
	UC2	0.011	108	1	0.002	1.12	0.239	0.0060	81.9	32.1	0.0032	2.25	2.96	9.80	1041	0.01	0.1	0.3	2780	0.97	0.32	0.52	1.55	1.03	3.10	1.45	1.48	4.0	11.7
	UC3	0.015	86	1	0.002	1.26	0.369	0.0068	63.9	23.5	0.0032	2.22	2.97	9.80	1041	0.01	0.1	0.3	3817	0.33	0.11	1.54	4.61	3.07	9.21	1.12	1.15	5.1	15.1
Figure 2B	UC1	0.012	79	1	0.002	1.14	0.248	0.0066	60.3	23.5	0.0032	1.95	2.57	9.80	1041	0.01	0.1	0.3	1575	0.57	0.19	0.87	2.61	1.74	5.23	0.98	1.02	5.8	17.1
	UC2	0.017	103	1	0.002	1.32	0.445	0.0066	76.1	27.3	0.0032	2.54	3.44	9.80	1041	0.01	0.1	0.3	2402	0.81	0.27	0.62	1.86	1.24	3.72	1.28	1.31	4.5	13.3
	UC3	0.014	75	1	0.002	1.21	0.319	0.0070	56.1	21.1	0.0032	2.01	2.67	9.80	1041	0.01	0.1	0.3	2944	0.30	0.10	1.66	4.97	3.31	9.93	1.01	1.05	5.7	16.6
Line x on Figure 3A	UC1	0.015	96	1	0.002	1.27	0.382	0.0066	71.3	26.1	0.0032	2.37	3.18	9.80	1041	0.01	0.1	0.3	1506	1.04	0.35	0.48	1.44	0.96	2.87	1.19	1.22	4.8	14.2
	UC2	0.018	103	1	0.002	1.35	0.488	0.0068	75.2	26.6	0.0032	2.59	3.51	9.80	1041	0.01	0.1	0.3	2069	0.96	0.32	0.52	1.56	1.04	3.13	1.30	1.33	4.4	13.0
	UC3	0.011	64	1	0.002	1.11	0.230	0.0070	48.5	19.1	0.0032	1.72	2.25	9.80	1041	0.01	0.1	0.3	2650	0.21	0.07	2.36	7.07	4.71	14.13	0.87	0.91	6.6	19.2

NOTATION

A = amplitude of the deflections of pycnoclines between turbidity and contour currents;

B = bankfull channel width;

B_d = bottom drag coefficient;

B/H = aspect ratio;

C = layer-averaged suspended sediment concentration of the current;

C_d = drag coefficient;

C_f = friction coefficient [equal to $(u_*/U)^2$];

Cz_p = dimensionless Chezy friction (calculated via u_p divided by u_*);

c_c = maximum volume concentration

Fr = densimetric Froude number;

g = gravitational acceleration;

$g`$ = reduced density;

H = bankfull channel depth;

h = layer-averaged thickness of the turbidity flow;

h_1 = the upper layer thickness at rest condition;

$h_1^`$ = interface depth;

k_s = bed roughness height;

Ri = Richardson number;

S = average thalweg slope;

U_t = layer-averaged velocity of turbidity flow;

U_c = layer-averaged velocity of contour current;

UCs = unidirectionally migrating deep-water channels;

v_* = shear velocity of the current;

u_*/v_s = ratio of shear velocity to settling velocity;

u_p = peak velocity of the current;

V = velocity of nonlinear surges and solitary waves along pycnoclines;

ß = paleocurrent direction of nonlinear surges and solitary waves along pycnoclines;

v_s = settling velocity of characteristic grain size (computed by a pondered average of all grain sizes in suspension);

v_* = turbulent velocity;

W = Wedderburn number;

W^{-1} = new Wedderburn number (equal to $\frac{\eta_0}{h_1}$)

z_c = distance above the bed to the point below which c is roughly equal to the maximum volume concentration (c_c);

z_i = distance from the bed to the current interface (equal to H);

z_p = height of the downstream velocity maximum;

α = ratio between bed shear stress ($\mathcal{T}_i$) and interface shear stress ($\mathcal{T}_b$);

ρ_1 = density of contour current;

ρ_2 = density of turbidity current;

ρ_i = density of the interstitial fluid;

ρ_s = density of the particles;

ρ_w = ambient water density;

$\overline{\Delta\rho}$ = layer-averaged excess density of the current;

$\overline{\rho}$ = layer-averaged density of the current;

$\overline{\Delta\rho}/\overline{\rho}$ = layer-averaged fractional excess density of the flow, the relation between layer-averaged concentration and excess density (*RC*) is equal to $\overline{\Delta\rho}/\overline{\rho}$.

η_0 = maximum interference displacement